

Emissions of Fe(II) due to the undersea volcano of El Hierro

TFT Máster Oceanografía



Student: Carolina Santana González
Tutor: J. Magdalena Santana Casiano
Co-tutor: Melchor González Dávila
Department: Chemistry
Group: QUIMA-IOCAG
December 2013

Contents

	Page
1. Introduction.....	3
1.1. Iron in seawater.....	3
1.1.1. Redox changes	3
1.1.2. Solubility.....	4
1.1.3. Biological uptake	4
1.1.4. Complexation	4
1.1.5. Scavenging onto surface.....	5
1.2. Main contributions of iron in the area	5
1.2.1. Atmospherics inputs.....	5
1.2.2. Hydrothermal inputs.....	5
1.3. Submarine eruption of El Hierro.....	6
1.4. Objectives.....	6
1.5. Study place.....	7
2. Material and methods.....	7
2.1. Reagents.....	7
2.1.1. Iron stock.....	7
2.1.2. Luminol.....	8
2.1.3. Carrier.....	8
2.2. Sampling	8
2.2.1. Sample collection and fixation	8
2.2.2. Measurements.....	8
2.2.3. Technique.....	8
2.3. Instrumental procedure.....	9
2.4. Standards and calibrated.....	10
3. Results.....	10
3.1. Sample Analysis.....	10
3.1.1. March 2013.....	11
3.1.2. October 2013.....	12
4. Discussion	15
4.1. Atmospherically and terrestrial inputs enhanced iron concentrations at sea surface water.....	15
4.2. Solubility control by organic complexation.....	16
4.3. Effects in the resuspension of particles in the seabed.....	16
4.4. Changes in iron concentrations associates to the seawater pH anomaly.....	17
5. Conclusions.....	18
6. References.....	18

1. Introduction

Iron is the fourth most abundant element in the crust (O'Sullivan et al., 1995; Bowie and Achterberg., 1998; Anderson and Morel, 1982; Brand et al., 1983) and it is an essential micronutrient for the organisms (O'Sullivan et al., 1995; Martin et al., 1991; Bowie et al., 2004). However, its concentration in the open ocean is in trace amounts ($< 1.0 \text{ nM}$) (Bowie and Achterberg., 1998), due to its low solubility (Liu and Millero., 1999, 2002).

In certain oceanic regions, as the High Nutrient Low Chlorophyll areas (HNLC), iron is found to be the main limitation of primary production (D. R. Turner, 2001; Martin et al., 1991). This makes iron the trace metal more important in seawater (K. W. Bruland and E. L. Rue, 2001).

The largest sources of iron to the seawater are atmospheric dust deposition, river transport, hydrothermal inputs, regeneration of the continental shelf and subsurface waters enriched by upwelling (Bowie y Achterberg, 1998; Bowie et al., 2002; Ye et al., 2009). While processes as biological uptake, scavenging onto surface and precipitation remove iron from surface water (Bowie et al. 2002; Ye et al., 2009).

The Trade Winds carries material from Sahara to the west of the Atlantic Ocean (Spokes et al., 2001). Due to it, in the Canary current a strong signal of dissolved Fe (DFe) and Al is observed from the West African coast. Surface mean concentrations observed of DFe are 1.11 nM (Sarhou et al. 2003) and for total dissolved iron (TD-Fe) of 1.9 nM (Bowie et al. 2002). Also in the region of upwelling subsurface waters with chlorophyll maxima, which dilutes the atmospheric signal Al, Fe and Co occurs (Bowie et al., 2002) and a fraction of biogenic iron particles are found (Powell et al., 1995).

1.1. Iron in seawater

According to oxidation state iron in the marine environment is found as Fe(III) which is the thermodynamically stable form in oxic waters (O'Sullivan et al., 1995; Achterberg et al., 2001; Santana-Casiano et al., 1997; Bowie et al., 1998). However, their concentrations are extremely low because of its tendency to form oxy-hydroxides or colloidal matter (Bowie et al., 1998; Achterberg et al., 2001) which nucleate and precipitate from the solution (K. W. Bruland and E. L. Rue, 2001) and are poorly soluble (T. D. Waite, 2001). Total dissolved iron has a half-life in the ocean of 10-50 years (H. J. W. de Baar and J. T. M. de Jong, 2001). In surface water iron can be reduced by chemical or photochemical processes that allow measurable concentrations of Fe (II) (Bowie et al., 1998; Santana-Casiano et al., 2000; Rose and Waite, 2006) to be determined. This is thermodynamically unstable and is rapidly oxidized to Fe (III) by O_2 and H_2O_2 (González-Dávila et al., 2004; Santana-Casiano et al., 2004, 2006). This difference in the oxidation state affects to the speciation and the bioavailability of iron (O'Sullivan et al., 1995).

The concentrations of dissolved iron (II) in the open ocean are very low $0.02\text{-}2 \text{ nmolL}^{-1}$. It is due to the rate of oxidation under high oxygen concentration. In oxygen minimum zones, suboxic and anoxic waters oxygen concentrations can be around $300\text{-}3000 \text{ nmol.L}^{-1}$. In interstitial water of marine sediments concentrations are about $300 \mu\text{molL}^{-1}$ and hydrothermal fluids can contain as much as 3 mmolL^{-1} of dissolved iron (H. J. W. de Baar and J. T. M. de Jong, 2001). According to their state of aggregation, it is found as colloidal, particulate or labile form (Ye et al. 2009; Achterberg et al., 2001).

The different inputs, redissolution, aggregation, photoreduction, adsorption onto surfaces, colloid formation, oxidation, sinking, complexation, dissolution of complex, biological

uptake and remineralization processes modifies Fe concentrations, redox and aggregation state (Ye et al. 2009). These changes in the speciation of iron make its concentration difficult to be measured.

1.1.1. Redox changes

The concentration of Fe (II) dissolved in the photic zone and in deep water, depends on the rate of oxidation of Fe(II) which is a function of the oxygen concentration, the pH (Santana-Casiano et al., 2004, 2006; González-Dávila et al., 2004, 2006; Miller et al., 2005; Shi et al., 2012; Trapp and Millero, 2007; King and Farlow, 2000), the temperature, $[\text{HCO}_3^-]$, $[\text{H}_2\text{O}_2]$ concentrations (González-Dávila et al., 2004; Trapp and Millero, 2007; King and Farlow, 2000) and ionic strength (González-Dávila et al., 2004, 2006; Santana-Casiano 2004, 2006).

The production of reactive oxygen species through photo-oxidation of organic matter and by the oxidation of other trace metals reduces iron species in seawater (Baker and Croot, 2010). In the photic zone, it can convert 50-60% of the dissolved iron in reduced iron species (H. J. W. de Baar and J. T. M. de Jong, 2001). Therefore, the presence of reactive oxygen species (HO_2/O_2^- , hydrogen peroxide and HO^\cdot) controls the speciation (Santana-Casiano et al., 2000) and oxidation of iron (Santana-Casiano et al., 2000; O'Sullivan et al., 1995; González-Dávila et al., 2006).

1.1.2. Solubility

The solubility of dissolved iron in the ocean at seawater pH is low (Liu and Millero 1999, 2002; Baker y Croot 2010). However, the amounts of organic ligands in seawater are the main control path in soluble iron (Baker y Croot 2010). Fe(III) solubility increase 25% when it is organically complexed in seawater (Millero et al., 1995). Fe(II) is more soluble than Fe(III), in spite of it is rapidly oxidized in oxic water (seconds to minutes) by O_2 and H_2O_2 (González-Dávila et al., 2006; Kustka et al., 2005).

1.1.3. Biological uptake

Phytoplankton is capable of using only forms of dissolved iron and stored when is in excess (W.G. Sunda, 2001), so that the uptake of colloidal or particulate iron needs a thermal or photochemical solution (O'Sullivan et al., 1995, Bowie et al., 1998).

The Fe(II) is the most bioavailable form and can be taken directly by the phytoplankton and by metal ion transporters (Anderson and Morel, 1982). Despite soluble inorganic species of Fe (III) are also bioavailable, they are present in sub-optimal concentrations for the growth of phytoplankton (Brand et al., 1983). The organic forms of iron affect its iron bioavailability and vary in different groups of phytoplankton (Hutchins and Bruland., 1994).

1.1.4. Complexation

90-99% of dissolved iron in the ocean appears as Fe bounding organic ligand complex (K. W. Bruland and E. L. Rue, 2001). These ligands have different functional groups which include carboxylic acid, amines, thiols and hydroxyl groups, whose organic complexation affects bioavailability and toxicity of metals (Sander and Koschinsky, 2011). In seawater they are affected for its production, remineralization, complexation, dissociation, photolysis, biological uptake and sediment release (Ye et al., 2009). It could be bioavailable for the phytoplankton growth (Santana-Casiano et al., 1997). The organic compounds can form complexes with Fe(II) and Fe(III) according to the pH of the solution and therefore they will have the ability to stabilize organic compounds (Santana-Casiano et al. 2000; T. D. Jickells and L. J. Spokes, 2001). In the deep chlorophyll maximum the enhanced of dissolved iron levels

resulting from the excretion of ligand and/or regeneration of iron through organic matter degradation or ingestion of particles and consequent dissolution and release of bioavailable iron (Bowie et al., 2002). The complex formation will affect the free Fe(II) oxidation rate (Santana-Casiano et al. 2000) and its reactivity (Bennett et al., 2008; Sander and Koschinsky, 2011).

1.1.4. Scavenging onto surface

The main sinking of dissolved iron in seawater is the scavenging of soluble and colloidal iron (Johnson et al., 1997) and it is strongly affected by the chemical composition of the particle surface (Baker and Croot, 2010). The marine chemistry of Fe(III) is primarily dominated by hydrolyzed species, which it should have great affinity for organic functional groups onto particle surface (H. J. W. de Baar and J. T. M. de Jong, 2001;).

1.2. Main contributions of iron in the area

1.2.1. Atmospheric inputs

In the Canary region more than 90% of iron aerosol is from the Sahara (Ussher et al. 2010), that can supply colloidal or nano-particles of iron to the study site (Baker and Croot, 2010; Spokes et al., 2001). This is correlated with aluminum input (Powell et al., 1995) due to 3.5% in crustal is formed by iron (D. R. Turner 2001; Nishioka et al., 2013). This aerosol can transform into soluble iron, which is the most available form of iron (Baker and Croot, 2010; Nishioka et al., 2013). However, it is rapidly removed from surface waters by sinking (Ussher et al. 2010), biological uptake, adsorption and/ or passive aggregation (Sarhou et al., 2003). The estimated resident time to DFe is $17 \pm 8 - 28 \pm 16$ days (Sarhou et al. 2003), although its deposition change throughout the year (Rijkenberg et al., 2008; Bowie et al., 2002).

1.2.2. Hydrothermal inputs

Hydrothermal vent are an important source of metal to the ocean. The injection of large amounts of material with different size, texture and chemical composition is considered as a nutrients source to the sea (Mantas et al. 2011).

The emission of Magmatic gas and reduced species modify the carbonate system, decrease the dissolved oxygen concentrations and reduce pE and pH (Santana-Casiano et al. 2013) which favor the presence of Fe(II) and decrease its oxidation rate (Santana-Casiano et al., 2013). The mainly reduce species of Fe and S emitted are: Fe^{2+} , $\text{Fe}(\text{OH})^+$, $\text{Fe}(\text{OH})_2$, FeCl^+ , $\text{Fe}(\text{HCO}_3)^+$, FeHS , H_2S , HS^- , S^{2-} , SO_3^{2-} , S_x^{2-} , S_2O_3^- , $\text{S}_4\text{O}_6^{2-}$. They contribute to reduce the redox potential and dissolved oxygen in the system and also it should have formed a complex colloidal FeS which remain suspended in the water and that is changing as the pH, will solubilize and release the Fe (II) (Santana-Casiano et al., 2013).

The reduced metals in the presence of O_2 precipitate in various mineral forms, mainly oxy-hydroxide (H. J. W. de Baar and J. T. M. de Jong, 2001) forming massive deposits of iron and manganese. Typical concentrations of dissolved iron in hydrothermal vent are $1-3 \text{ mmolL}^{-1}$, with extreme value in Juan de Fuca Ridge about $18,7 \text{ mmolL}^{-1}$ (H. J. W. de Baar and J. T. M. de Jong, 2001)

In upwelling areas hydrothermal dissolved iron can reach the photic zone (Sander and Koschinsky, 2011; Severmann et al., 2004), and introduce particulate iron which can be redissolved by photoreduction (Severmann et al., 2004).

1.3. Submarine eruption of El Hierro

The eruption of the submarine volcano on the island of El Hierro occurred on October 10th, 2011 and it was the first submarine eruption in 600 year of historical record in the Canary Island (Becerril et al., 2013). The affected area covered the SE and NW of the island (Santana-Casiano et al., 2013). On October 23th, undertook the first survey in the volcanically area and the base of the active volcano was found at a deep of 350 m at 27°37'07"N - 017°59'28"W. The volcano was located on a rift with the lava flowing south-westward. The volcano was 650 m wide and its peak was situated at a depth of 220 m below sea level. In January 2012, the cone had risen to a depth of 130 m and in February it reached its maximum elevation of 88 m below sea level. While both the structure and the height of the volcanic edifice were changing, the emission plume was also being modified (Santana-Casiano et al., 2013).

During eruptive stage it was emitted large amounts of material with size, texture and chemical composition variable, magmatic gases and reduced chemicals species (Santana-Casiano et al., 2013). Moreover benthic species in the area were buried. This emission caused a change in physical-chemical properties in the region of principal cone, such as decreasing pH and dissolved oxygen. Anoxic conditions were reached in the region nearest the main cone. This generated death in pelagic communities (Fraile-Nuez et al., 2012).

In addition there was an increase in temperature, with maximum anomaly of 18.8°C at 210 m depth (Fraile-Nuez et al., 2012), C_t (total dissolved inorganic carbon) of 2100 $\mu\text{mol/Kg}$ up to 7682 $\mu\text{mol/Kg}^{-1}$ and A_t (total alkalinity) of 1338 $\mu\text{mol/Kg}^{-1}$ in surface water around the volcano (Santana-Casiano et al., 2013). The carbonate system in the seawater was strongly affected and its buffer capacity was dramatically reduced. The important increase in $p\text{CO}_2$ to 223000 μatm values made the area acts as CO_2 source to the atmosphere (Fraile-Nuez et al., 2012).

Fe(II) concentrations increased to 50 μM and pH decreased to 5.1 (Fraile-Nuez et al., 2012; Santana-Casiano et al., 2013). This contributed to the acidification of the system by reaction of Fe(II) with H_2S (equation 1). Nutrient supply was also determined, acting as a natural fertilizer for the subsequent natural recovery of the ecosystem (Fraile-Nuez et al. 2012; Mantas et al. 2011; Santana-Casiano et al., 2013). The changes generated by the emission can serve as a possible stage for ocean acidification (Fraile-Nuez et al., 2012; Santana-Casiano et al., 2013).



The eruptive stage ceased on March, 2012 and the system evolved to hydrothermal. The physical-chemical properties were returned to normal conditions, except in 0.5Km around of the main cone where pH and C_t were anomaly (Santana-Casiano et al., 2013).

1.4. Objectives

This work focuses on the study of variation in concentrations of dissolved Fe(II) due to emissions from undersea volcano on the island of El Hierro after the eruptive process. To determine the concentration of Fe(II) flow injection chemiluminescence using luminol as reagent was used. The study of the temporal evolution of the dissolved Fe(II) concentrations after the eruptive process in submarine volcano, give information on the process of fertilization occurred in the area providing information that will evaluate the system recovery.

1.5. Study place

The study was conducted in the region of the undersea volcano, southwest of the municipality of La Restinga, on the island of El Hierro, during the oceanographic cruise VULCANO on board the R / V Ramón Margalef and B / V Ángeles Alvariño on March and October 2013, respectively. A grid and a high-resolution sub-grid of stations were performed with oceanographic rosette.

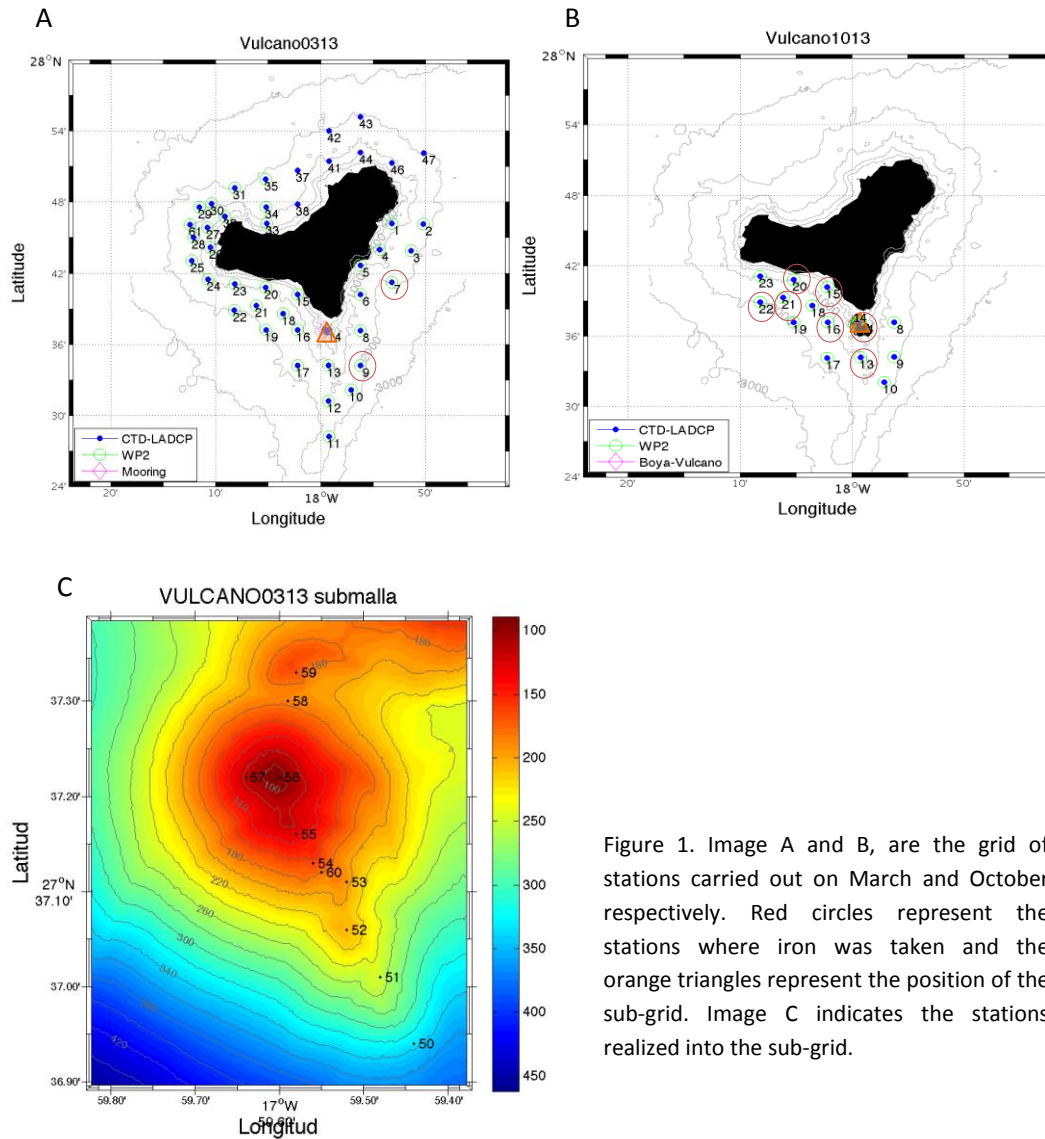


Figure 1. Image A and B, are the grid of stations carried out on March and October respectively. Red circles represent the stations where iron was taken and the orange triangles represent the position of the sub-grid. Image C indicates the stations realized into the sub-grid.

2. Material y methods

2.1. Reagents

Reagents were prepared with deionized ultrapure water (milli-Q).

2.1.1. Iron stock

An iron stock of $6,211 \times 10^{-4}$ M was prepared using ammonium iron(II) sulphate hexahydrate (SIGMA-ALDRICH). HCl (previously quartz distilled) was added to the water to

lower the pH to 2 and retard any oxidation. Then it was stored in the dark until use. A diluted stock was prepared with concentration of 2.416×10^{-6} M.

2.1.2. Luminol

The luminol was prepared using 0.24875 g of 5-amino-2,3-dihydro-1,4-phthalazinedione (FLUKA), 26.49757 g of Na_2CO_3 (SIGMA-ALDRICH) and 188.175 ml of NH_3 (PANREAC)(previously distilled) in 5 l and it was adjusted to pH 10.0 by adding 6M Q-HCl. At this pH the luminescence is optimal (Bowie and Achterberg, 1998). The luminol solution was stored in dark due to its light sensitivity. To ensure the complete dilution, it was prepared days prior to use. The solution became more stable 24 hours after preparation and for at least a month after (King et al., 1995).

2.1.3. Carrier

The carrier used was NaCl 0.7 M to get an ionic strength similar to that of seawater in standards and samples. In this analysis, milli-Q water was used as a cleaner in the injection system. Furthermore, dilute HCl at specific moments when capillaries were obstructed or contaminated was used (e.g. if the injection pump recedes sample).

2.2. Sampling

2.2.1. Sample collection and fixation

Samples were taken with niskin bottles in almost all stations and with go-flo bottles in stations nearest to the volcano cone. Acid pre-cleaned polyethylene containers were used and fitted with 45ml of unfiltered sample. Previous to sampling 10 μ l of HCl (6M) was added in order to keep the seawater solution at pH 6.

2.2.2. Measurement

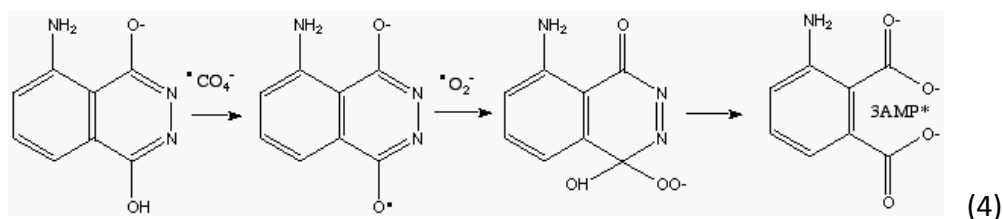
The samples were analyzed *in situ*. They were fixed to pH 6 and stored in the refrigerator until analysis. This treatment decreases the oxidation of iron (González-Dávila et al., 2004). Before analysis, the sample was tempered before the injection into the system.

A SBE 18 pH sensor was used to automatically record pH profiles attached to the SBE 9Plus CTD rosette with 24-12 liters bottles. pH values are expressed as pH in NBS scale at *in situ* conditions. It uses a pressure-balanced glass-electrode /Ag/AgCl-reference pH probe to provide *in situ* measurements at depths up to 1200 meters. The pH sensor was calibrated against precision buffer solutions of 4, 7, and 10 pH \pm 0.02 pH.

2.2.4. Technique

The technique used in this study in order to determine the concentration of Fe(II) was the chemiluminescence technique using luminol as the reagent, following the method of King et al (1995) for use in seawater. The method is based on the detection of light generated by the reaction of Fe(II) with oxygen in the presence of luminol (5-amino-2,3-dihydro-1,4-phthalazinedione).

Ferrous iron is oxidized by dissolved molecular oxygen to produce superoxide (equation 2), and subsequently the peroxy carbonate radical (equation 3). These species oxidize luminol in two steps to produce luminescence (equation 4).



The oxidation of luminol produces a blue color luminescence with maximum emission wavelength at 425 nm. The intensity of luminescence generated by the luminol is often modified by the presence of certain metal ions, but in seawater with oxic conditions these concentrations are too low to cause significant interferences (Handsard and Landing, 2009).

This technique has been widely used by several authors (O'Sullivan et al., 1995; King et al., 1995; Bowie et al., 1998, 2003, 2004, 2006; Handsard and Landing., 2009; Powell et al., 1995) due to the many advantages offered as high selectivity (Handsard y Landing 2009; Achterberg et al., 2001); simple, rapid and inexpensive detection (Handsard y Landing, 2009; Achterberg et al., 2001; Powell et al., 1995); can be performed in laboratory vessel (Bowie et al. 1998; Achterberg et al., 2001); low detection limit (Bowie et al. 1998; Powell et al., 1995) and multiple analysis (Powell et al., 1995).

2.3. Instrumental Procedure

Waterville Analytical instrumentation uses flow injection analysis, FIA, to deliver a sample to a flow cell where analyte-specific chemiluminescence occurs. Analyte specificity is achieved by careful selection of the chemiluminescent reagent and analytical conditions such as: reaction pH, reaction time, and masking reagents.

Before being used all the materials was rinsed three times with distilled water, three times with milli-Q water and stored in 10% HCl solution for cleaning. When the material was going to be used, it was rinsed three times with distilled water and three times with milli-Q water. After the analysis, the material was cleaned and re-stored in the HCl solution. This way we avoided the contamination of containers that were used.

In the first place the four hoses are placed in the peristaltic pump (Rainin Dynamax 15.8 V) which is previously connected to the detector. Subsequently the pressure is regulated in the hoses while water milli-Q passes one by one. This allows the flow to be uniform and not by pulses. After adjusting the proper pressure hoses the water cleaning mode was allowed during 3 mins. After this time we let some air to pass and we put each hose into the corresponding receptacles: luminol, NaCl, milli-Q water and sample. The Software executed in the chemiluminescence was provided by Water analytical (WA CONTROL V105, PHOTO COUNTER CONTROL). The analytical time selected was 100 seconds that allowed the full record of the peak signal. The peak area mode was selected in order to compute the signal. Three measurements for each sample were carried out and values were presented as average values. After a set of analysis, milli-Q water was allowed to clean all hoses, and finally air was run to empty them.

Every day three standards were performed to ensure that the initial calibration was maintained.

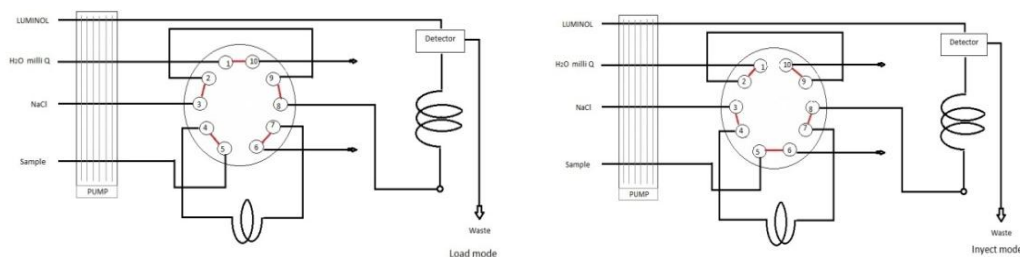


Figure 2. Instrumental diagram

2.4. Standards and calibrate

Seawater used in the calibration procedure was taken from the place of the study in a station no affected by the volcano and aerated with a magnetic stirrer during 60 mins in atmospheric contact. This time was sufficient to achieve complete oxidation of Fe(II) (González-Dávila et al., 2004; Handsard and Landing, 2009) and the matrix of the sample was maintained, following the procedure carried out by Handsard and Landing (2009).

25 ml flasks to which 10 μ l of 6 M HCl was added were used in the study. The required diluted iron stock was added to reach the final concentration and the flask was filled with aerated seawater. The pH in the flask was 6. A blank without the addition of iron is done in each calibration step. A linear regression was achieved and the concentration of the sample, TDFe(II), was estimated. TDFe(II) included the forms of Fe(II) in the dissolved, colloidal and labile phases.

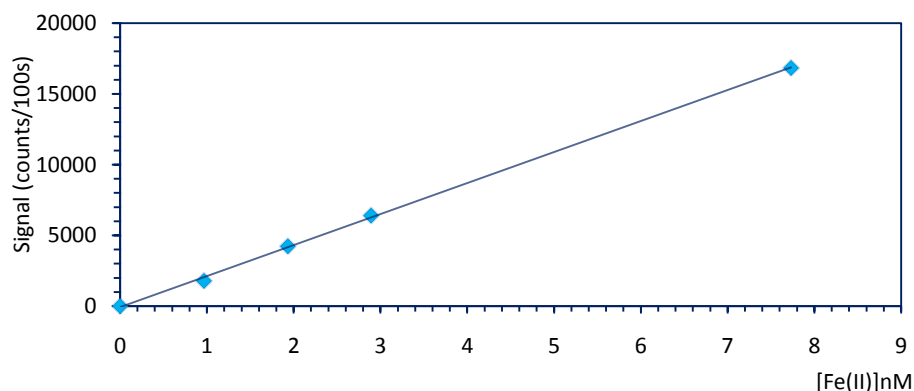


Figure 3. Calibration curve.

The calibration curve used was made in the concentrations range 0.966-7.7312 nM with correlation coefficient $r^2 = 0.999$. Moreover in other calibrations realized before in land base laboratory linearity was obtained to 100nM of iron. The detection limit obtained was 0.09 nM ($LD = 3 \times STD [Blank]$, $n = 4$).

3. Results

3.1. Sample Analysis

In this work it is reported TDFe(II) concentrations analyzed during two cruises, in March and October, 2013. Moreover pH and fluorescence data were depicted in most of the stations. During the March cruise two stations outside the influence zone of the volcano and nine stations along the volcano transect were analyzed with niskin and go-flo bottles, respectively. In the October cruise seven stations outside of the volcano influence zone and eleven stations into the volcano transect were analyzed.

3.1.1. March 2013

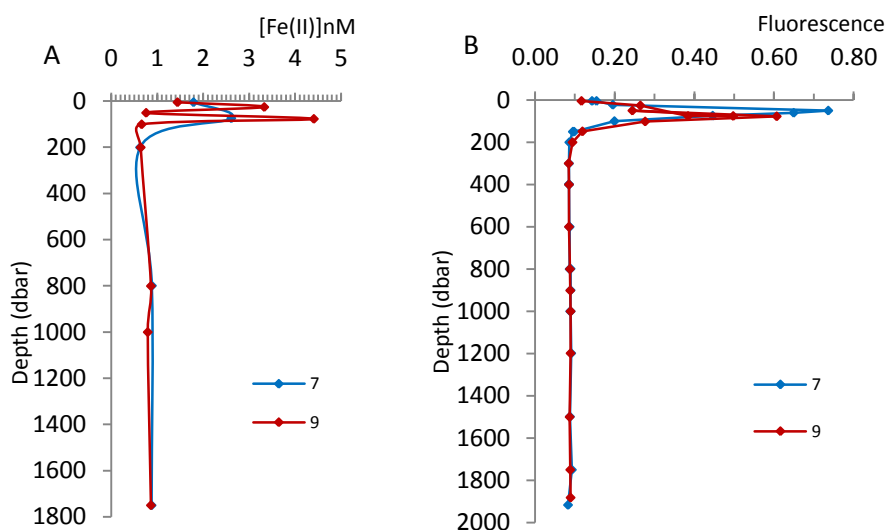


Figure 4. Image A represents 2 profiles of TDFe(II) concentrations in regions outside of the volcano influence taken with niskin bottles. Image B represents the same profiles of fluorescence obtained with a fluorometer sensor.

In fig. 4 A, the concentrations of TDFe(II) observed in sea surface water were 1.79 nM for the station 7 and 1.44 nM for the station 9. At station 7 an iron peak maximum of 2.61 nM at 74 dbar was observed. Below 200 dbar the concentration remained nearly uniform to the sea bed with values of 0.63 – 0.86 nM. However in station 9, located southern of the volcano site, 2 iron peaks maxima were observed with values of 3.32 nM and 4.40 nM at 25 and 77 dbar respectively. The chlorophyll profiles, in fig 4 B, reflected the deep chlorophyll maximum (DCM) located in both stations between 25-75 dbar. At the station 7 the chlorophyll peak was observed at the same depth that for the Fe(II) concentration. Two chlorophyll peaks were also observed at station 9, similar to the distribution observed for the iron concentration in the same station. These high Fe(II) values indicated an important source of Fe(II) in the area that could be kept in solution due to organic complexation by exudates of algae at the chlorophyll maximum.

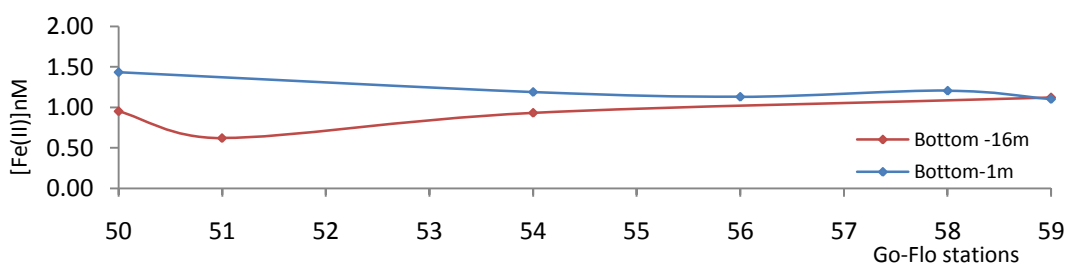


Figure 5. TDFe(II) concentrations in station into volcano transect and they were taken with go-flo bottles at 1m and 16m from the bottom. The main cone is located at station 56.

Values in iron(II) concentrations along the volcano transect, fig. 5, near the bottom were around 1.1 nM, with a slight higher value around the station 50, reaching 1.4 nM. Samples taken 15 m above the bottom sample presented always a lower value, in the 0.6 - 1.1 nM range. These observations along the section reflected that during the time the section was sampled there was not any significant emission of iron by the volcano or, the section was out the influence of any Fe(II) volcano source. The differences in TDFe(II) observed in Figure 5 may be due to redissolution from the bottom.

3.1.2. October 2013

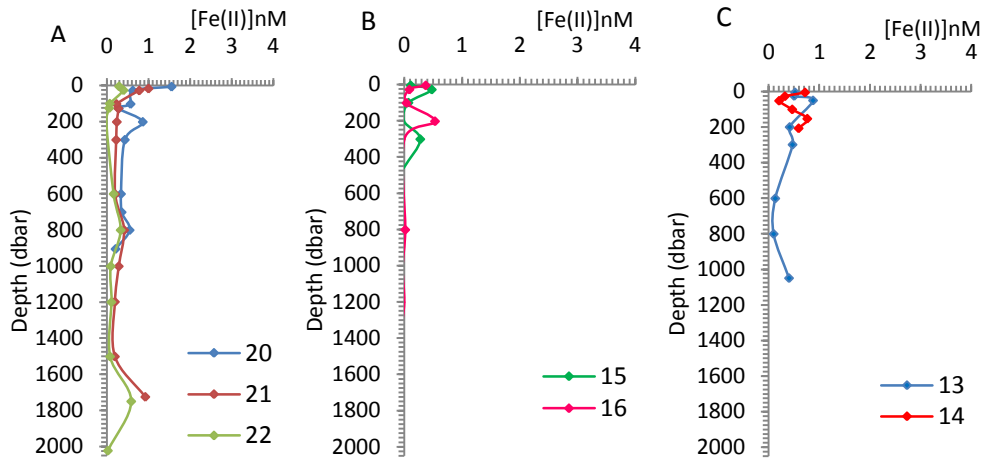


Figure 6. Profiles of TDFe(II) concentration at stations nearest the volcano influence zone. It was taken with niskin bottles. In the image A the stations are located western, in the image B the stations are located between western stations and the volcano zone and in the image C the stations are located in the same longitude which volcano.

In fig. 6 profiles show that in sea surface water concentrations of TDFe(II) were lower than 1.55 nM. At stations 22, 15 and 13 a light increase in iron concentration was observed between 25 - 50 dbar. At stations 20, 16 and 14 this increase was observed at around 200 dbar. Iron concentrations near the bottom were lightly enhanced up to 0.9 nM, possibly due to redissolution or resuspension of material from the bottom. These stations were located in the insular slope.

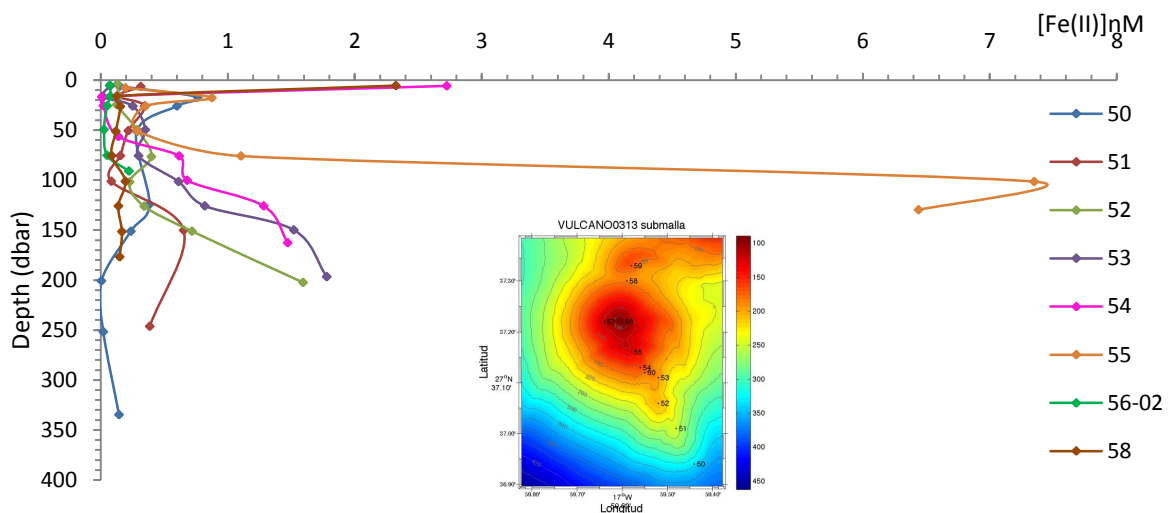


Figure 7. Profiles of TDFe(II) concentrations in the sub-grid stations into the volcano transect. Samples were taken with niskin bottles.

Figure 7 shows the in iron(II) concentration along the volcano sub-grid section. The sea surface waters presented low Fe(II) concentration, with values of around 0.2 nM. However, stations 54 and 58 presented surface values that reached 2.72 and 2.32 nM, respectively. An enhanced iron concentration was observed at 25 dbar for all the stations, associated to the maximum in chlorophyll a in the section. All the stations presented an important increase in their concentrations from 50 dbar to the bottom depth, with the exception of the southernmost station, St. 50 that only showed a small increase reaching 0.2 nM. Values between 1.5 and 1.8 nM were measured at the bottom (160 -200 dbar) for stations 52, 53 and 54. The maximum TDFe(II) concentration of 7.34 nM was measured at 100 dbar in station 55. The TDFe(II) concentration decreased as we moved away from station 55. In the main cone, station 56-02 was, the TDFe(II) concentration was only 0.22 nM and in station 58 was 0.14 nM.

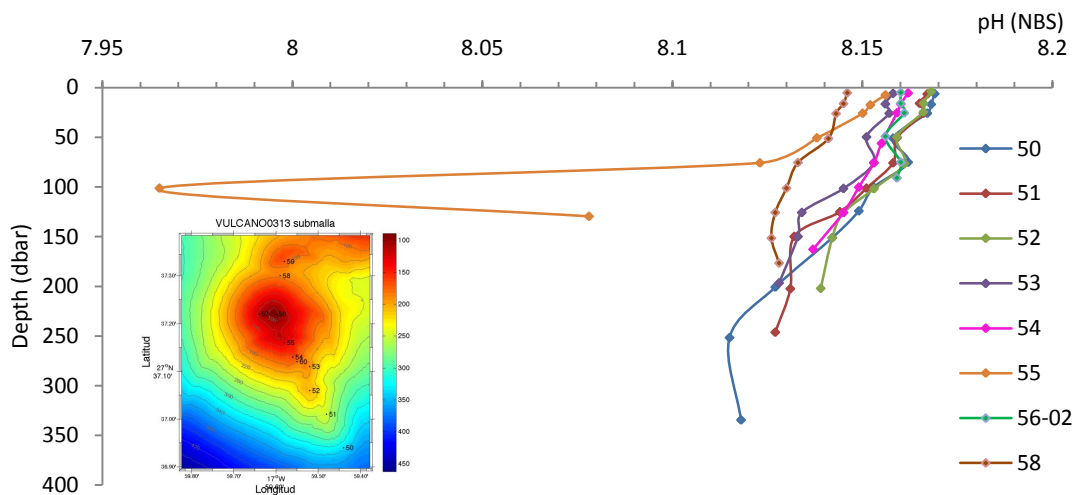


Figure 8. Profiles of pH (NBS) in the sub-grid stations along the volcano transect.

Figure 8 depicts the pH at *in situ* conditions along the volcano sub-grid. At the sea surface the values were 8.16, except in the station 58 which reach 8.14. All the stations presented a decrease in pH values from 50 dbar to the bottom. However, values were 0.01 to 0.02 units lower than those observed at station 50. The minimum pH values was measured at station 55, with a pH of 7.96 at 100 dbar, a value 0.2 units lower than the value in station 50. This value increased as we moved away from station 55.

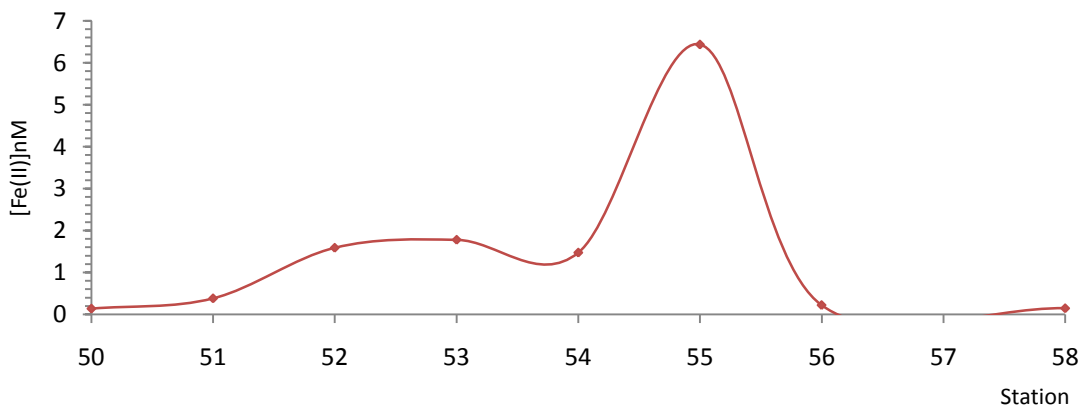


Figure 9. TDFe(II) concentrations in the bottom of sub-grid stations into the volcano transect. It was taken with niskin bottles. The main cone is station 56.

Figure 9 shows the concentrations of iron at the bottom depth along the transect. Two iron anomalies were observed. The first between station 52 and 53, where values of 1.59 nM and 1.77 nM were obtained, respectively, and the second at station 55, where a concentration of 6.44 nM was obtained.

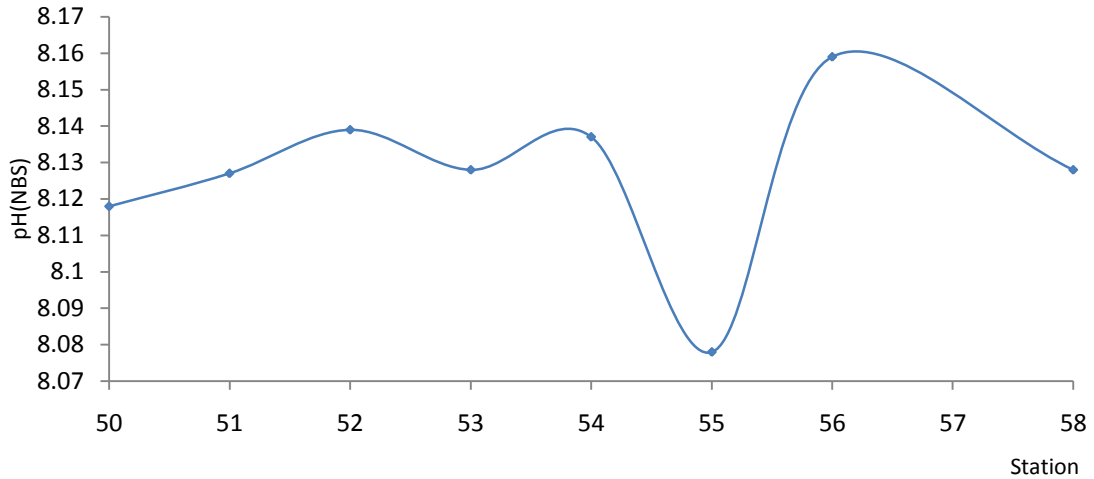


Figure 10. pH (NBS) in the bottom of sub-grid stations into the volcano transect.

Figure 10 shows the pH at *in situ* conditions for the bottom samples in the whole transect. A trend opposite to that showed by the concentration of iron(II) (fig. 9) was observed. A decrease in pH values was observed at station 55 with a pH value of 8.078, the lowest for the section. Moreover, a slightly decrease in pH was also observed in stations 53 with a value of 8.12 (which presented a value lower than adjacent stations) and stations 50, 51 and 58 with values of 8.118 nM, 8.127 nM and 8.128 nM, respectively.

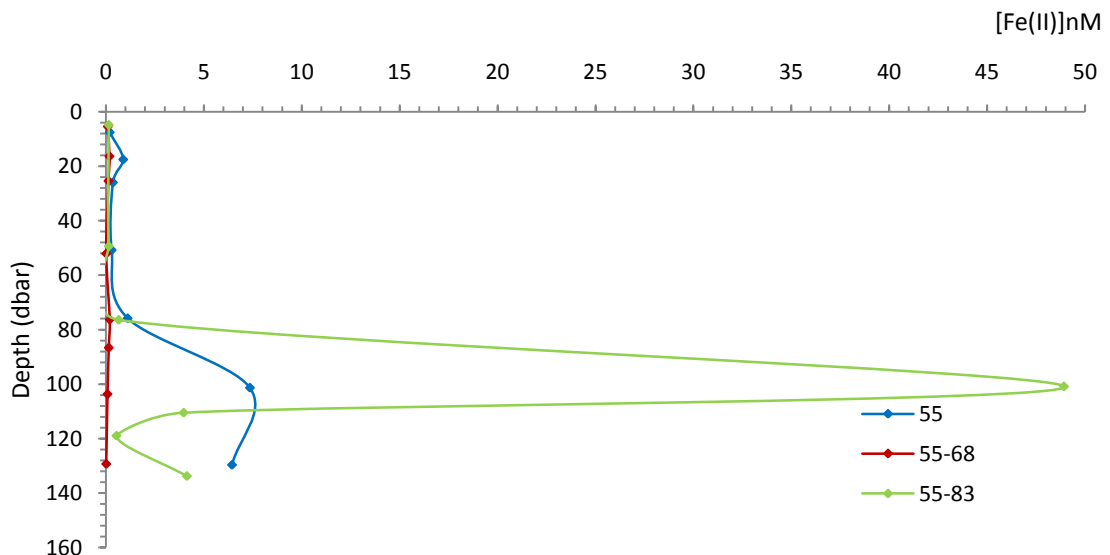


Figure 11. Fe(II) concentration in station 55 into the sub-grid at three different moments. The stations 55, 55-68 and 55-83 were taken with niskin bottles on November 3th, 5th and 7th respectively.

Station 55 was sampled three times at different hours and days for Fe(II), following a yo-yo study. The Fe(II) profiles for stations 55, 55-68 and 55-83, with 2 days between them, are plotted in Figure 11. An important iron anomaly was observed at 100 dbar. This anomaly was 7.34 nM on 3th November and it reached 48.92 nM on 7th November. However any anomaly

were detected on 5th November, where concentrations were lower than 1.4 nM at the same depth.

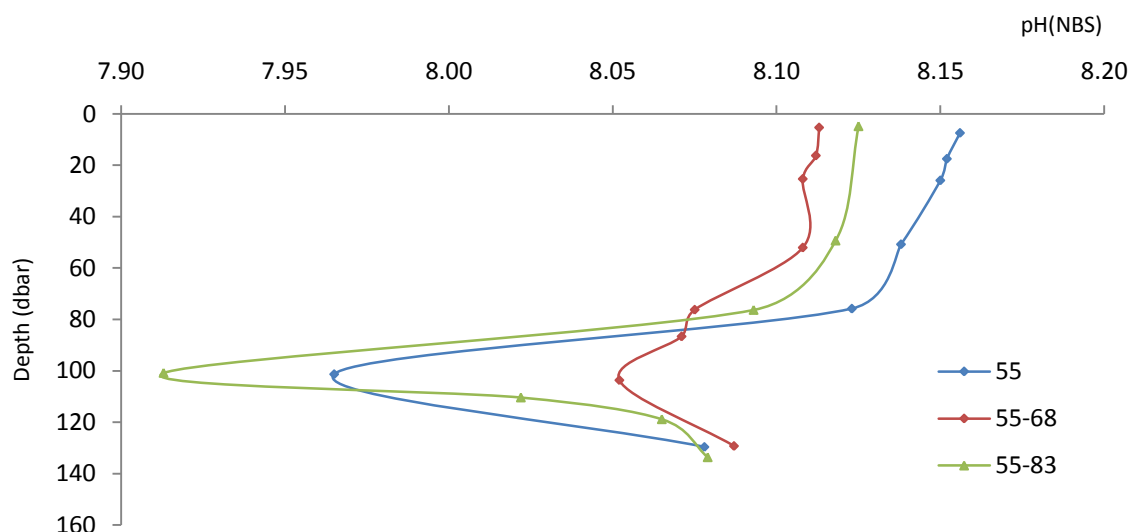


Figure 12. pH (NBS) in station 55 into the sub-grid at three different moments. The stations 55, 55-68 and 55-83 were taken on November 3th, 5th and 7th respectively.

Figure 12 shows the pH profiles for the stations 55, 55-68 and 55-83 that also revealed important pH anomalies at 100 dbar, where pH decreased by 0.2 units, reaching a value of 7.91. On November 3th, the pH value was 7.96, a decrease of 0.15 units. On November 5th the pH anomaly was slightly lower, with a pH value of 8.02 and on November 7th, the anomaly in pH became more important, reaching a pH value of 7.91.

4. Discussion

4.1. Atmospherically and terrestrial inputs enhanced iron concentrations at sea surface water

In the Canary region the atmosphere plays an important role in material transport from land to the sea. This is due to this area is affected by dust deposition from Sahara desert that enhanced iron concentrations in sea surface waters. Moreover, most of the stations sampled both during March and October 2013 cruises are located inside 5 miles around the island of El Hierro, providing the island itself an additional source of particulate and soluble iron to the surrounding seawater. During March (fig. 4, A) and October (fig. 6 and 7) cruises relatively high iron concentrations in surface water were observed. This enhancement could be associated to the island effect and to atmospheric inputs from the vicinity of Sahara west coast (Ussher et al., 2010) that can supply colloidal particles of iron associated with coarse-mode aerosol (Spokes et al., 2001; Baker and Croot., 2010) and photo-chemical processes allow measurable concentrations of Fe(II) in surface waters (Santana-Casiano et al., 2000). These sources can supply important amounts of colloidal or nano-particulate iron which can be transformed via post-depositional processes into soluble Fe (Baker and Croot., 2010) which is the most bioavailable form of iron (W.G. Sunda, 2001). On the one hand during March cruise (fig. 4 A) sea surface total dissolvable iron concentrations were a bit higher than on October cruise (fig. 6) which could be explained due to higher surface runoff from the island of El Hierro and associated to the late winter rain. On the other hand the maximum concentrations of TDFe(II)

observed in this study were 1.79 nM. Previously in Atlantic Eastern at Canary current were reported DFe ($< 2 \mu\text{m}$) of 1.9 nM (Bowie et al., 2002), 0.7 nM (Ussher et al., 2010) and 1.11 nM (Sarhou et al., 2003) which include the oxidations state +2 and +3. These values are in the same order than values found in this work although different fractions of iron were measured and the redox state.

4.2. Solubility control by organic complexation

In the ocean Fe(III) is the thermodynamic stable form of iron and its solubility is very low (Liu and Millero., 1999, 2002), but in the presence of organic matter the Fe(III) can be reduced to Fe(II) (Santana- Casiano et al., 2000 and 2010). In this study during March cruise (fig. 4, A) three peaks (one at station 7 and two at station 9) of high TDFe(II) concentrations were observed between 25 and 77 dbar coinciding with the chlorophyll maximum (figure 4, B).

These signals in iron concentrations and in fluorescence may be associated to organic ligands excretion by phytoplankton (Gledhill et al., 2004) that can strongly influence the redox chemistry of this metal (González-Dávila, 1995). The organic ligands can play a key role in keeping Fe, which is released from the colloidal Fe(III) present in solution (Rijkenberg et al., 2008). The presence of organic ligands not only change the speciation of iron also modified the ratio between iron and other essential or non- essential trace metal which affects the uptake of iron depending on the synergist or antagonist effects of different alga specie present in the area (Santana- Casiano et al., 1997). The complexes formation is function of the pH and the ligand stabilization capacity (Santana-Casiano et al., 2000) which will affect the oxidation state of Fe and to the oxidation rate of Fe(II) in seawater (Santana-Casiano et al., 2000). Minimal dissolved Fe are often associated with depth of chlorophyll maximum Bergquist and Boyle, 2006; Bowie et al., 1998). However the pattern observed in this work has seen previously obtained by Bowie et al., (2002) close to the subtropical convergence zone in the southwest Atlantic, in the Guinea oligotrophic gyre in the southeast Atlantic and in the northwest African upwelling zone, with shallow chlorophyll a maxima and enhanced Fe concentrations above the thermocline.

Other possible explication for the high signal in fluorescence and enhanced TDFe(II) may be the regeneration of iron through degradation of organic matter or ingestion of particles and subsequent dissolution and release of bioavailable iron (Hutchins and Bruland, 1994).

In the deep open ocean an average concentration of 0.7 nM dissolved Fe exist (Bergquist and Boyle, 2006a) in association with Fe binding ligands that are present in concentrations ranging from 0.7 to 1.4 nM. These values are according with values reported in this work at stations out the volcano influence zone.

4.3. Effects in the resuspension of particles in the seabed

The samples near the bottom showed a light enhance in iron concentrations (fig. 5 and 6(A and C)). This could be due to the resuspension of material from the bottom resulted from the 2011 eruptive process (Zhang et al., 2013; Bonnin et al., 2006; O'Hara Murray et al., 2012) which it is influenced by the turbulence generation (O'Hara Murray et al., 2012).

In fig. 5 iron concentrations changed in the different sub-cones and with a difference in deep of 15 m each other. Samples taken 1 m from the bottom TDFe(II) concentrations are between 1.1 -1.4 nM and in samples taken 16 m from the bottom are between 0.6-1.1 nM.

Both samples showed the same concentration range, but it was detectable a slightly increase in samples taken nearest to the bottom. The Fe concentrations are highest near its sources, and concentrations decrease rapidly with distance from sources due to the reactivity and insolubility of Fe in seawater (Johnson et al., 1997). Another source of iron which could be contributing to this enhanced bottom concentrations is the input from hydrothermal vent. The range of concentrations observed during March 2013 are much lower than those observed during October 2013 cruise, but differences in the currents regime could explain the most homogeneous distribution observed in March with respect to that in October (see below).

4.4. Changes in iron concentrations associates to the seawater pH anomaly

In the sub-grid stations into the volcano transect (Fig. 7) during October 2013, an anomaly in the profiles of iron concentrations, was observed. In surface TDFe(II) values were lower to 0.4 nM, except the stations 54 and 58 where samples values exceeded 2.3 nM. Station 58 presented a relatively low pH values profile along the full depth which could be associated to CO₂ emissions from hydrothermal vents located in the volcano area.

During October 2013, the anomalies in the iron concentration were detected since 50 dbar depth to the bottom. The gradual increase in iron concentrations with depth reached the maximum concentration of iron of 7.34 nM at 100 dbar in the sub-cone located in the station 55 and then iron concentrations decreased once this cone was passed. The iron concentration anomaly was also followed by an important anomaly in the pH signal (Fig. 8) at the same profile transect and at the same depth, with an opposite behavior. The pH values decreased through transect from station 50 to station 55, where the minimal signal at 100 dbar with pH of 7.96 was measured. The concentrations of iron (fig. 9) and the pH signal (fig. 10) also showed a mirror image in the bottom values across the volcano transect. The increase in TDFe(II) concentration at station 55 coincided with a decrease in pH and the increase in TDFe(II) between stations 52 and 53 was observed at pH signal in the station 53. This relationship between low pH (high values of total dissolved inorganic carbon were also measured, data not shown) and high TDFe(II) concentration indicated that emission of hydrothermal fluids were present in the area, in particular in the proximities of the station 55 which were affecting the pH and TDFe(II) profiles and the bottom values.

In order to detect a possible temporal change in the values studied at station 55, a yoyo sampling was done (Fig. 11 and 12). A temporal change in iron concentrations and pH values were observed. The TDFe(II) profiles at station 55 (Fig. 11) changed with a temporal difference of two days between them, along four day of study, which were especially greater at 100 dbar depth. During this yoyo stations a drastic change was observed with values from 1.4 nM to 48.92 nM of TDFe(II). The same anomalies were detected in the pH values (fig. 12) which an oscillation of pH from 8.05 to 7.91 and both anomalies coincided in the time. The anomalies in pH and TDFe(II) concentrations confirmed the emission of gasses in the volcano region, especially in the sub-cone located at station 55, a process that can be defined as an intermittent event of hydrothermal fluids, rich in CO₂ and, at least, in iron reduced forms, which is affecting the surrounding volcanic area, which can favor an increased biological activity as result of this natural fertilization event.

The effect of low pH values would also favor the high anomaly in TDFe(II), because of iron(II) concentrations is pH dependent (Liu and Millero, 1999; González-Dávila et al., 2004). When pH decrease the oxidation rate of iron is also decreased (Santana-Casiano et al., 2004) and it allows maintaining Fe(II) in solution for periods of time larger than that at normal pH of

the seawater (Santana-Casiano et al., 2004; Statham et al., 2005). The emission of iron and nutrients (Santana-Casiano et al., 2013) increase the rate of phytoplankton production (Martin et al., 1994; Fitzwater et al., 1996) which induced changes in organic iron complexation and Fe(II) oxidation rates favored at the low pH values in the area (Breitbarth et al., 2010). Iron-ligands complexes have been found in the seawater fluid plumes rising above the vents (Bennett et al., 2008; Statham et al., 2005) which stabilize metals in hydrothermal fluids (Sander and Koschinsky, 2011) and will reduce the reactivity of the Fe species, preventing precipitation of Fe and scavenging into/onto particulate phase (Bennett et al., 2008). Authors such as Breitbarth et al., (2010) observed that ocean acidification may lead to enhanced Fe-bioavailability due to an increased fraction of dFe and elevated Fe(II) concentrations in coastal systems. Moreover seawater pH affects phytoplankton physiology (Fu et al., 2008) and thus indirect effects via phytoplankton exudates that complex iron may also alter biological influence on iron solubility and cycling (Breitbarth et al., 2010).

5. Conclusions

Two cruises were carried out during March and October 2013 south of the Island of El Hierro in the area affected by the 2011 submarine eruptive process in order to study the temporal evolution of the dissolved Fe (II) concentrations and gather information about the fertilization process in the area. The luminol based chemiluminiscent technique was used in order to detect natural total dissolvable Fe(II) concentrations. The area out of the influence of the volcano presented TDFe(II) concentrations in the range between 0.2 to 2 nM typically found in North Atlantic profiles, with maximum values at the surface associated to chlorophyll *a* maximum and to the sea bottom, showing the important influence of surface runoff, organic complexation and particle re-suspension processes. Important deviations were observed in the proximities of the volcano during the October 2013 cruise. TDFe(II) positive anomalies were followed by negative anomalies in pH along the full profiles and for the bottom samples. These effects indicated the emission of hydrothermal fluids in the area, in particular in the proximities of the station 55, in a secondary cone, which affected the pH and TDFe(II) profiles and the bottom values. The temporal study at St 55 during 4 days showed an important variability in both pH and TDFe(II) concentration that indicated the volcanic area was affected by intermittent events of hydrothermal fluids in vent that remains in the volcano cone one and a half year after the eruptive phase has ceased. The increased TDFe(II) concentrations and the low associated pH values may be acting as an important fertilization event in the seawater around the volcano at the Island of El Hierro providing optimal conditions for the regeneration of the area.

Acknowledgements

This work was supported by the Spanish Government, Ministerio de Economía y Competitividad, through the projects ECOFEMA (CTM2010-19517) and VULCANO (CTM2012-36317).

6. References

Achterberg E.P., Holland T.W., Bowie A.R., Mantoura R.F.C., Worsfold P.J. Determination of iron in seawater. *Anal Chim Acta* 2001 8/31;442(1):1-14.

- Anderson, Michael A. and Morel, Francois M. M. The influence of aqueous iron chemistry on the uptake of iron by the coastal diatom *thalassiosira weissflogii*. *Limnology and Oceanography* 1982;27(5):789-813.
- Baker A.R., Croot P.L. Atmospheric and marine controls on aerosol iron solubility in seawater. *Mar. Chem.* 2010 6/20;120(1-4):4-13.
- Becerril L., Cappello A., Galindo I., Neri M., Del Negro C. Spatial probability distribution of future volcanic eruptions at RI Hierro Island (Canary Islands, Spain). *J. Volcanol. Geotherm. Res.* 2013 5/1;257(0):21-30.
- Bennett S.A., Achterberg E.P., Connelly D.P., Statham P.J., Fones G.R., German C.R. The distribution and stabilization of dissolved Fe in deep-sea hydrothermal plumes. *Earth Planet Sci. Lett.* 2008 6/30;270(3-4):157-67.
- Bergquist B.A., Boyle E.A. Dissolved iron in the tropical and subtropical Atlantic ocean. *Global Biogeochemical Cycles* 2006;20:1-14.
- Bonnin J., Van Haren H., Hosegood P., Brummer G.A. Burst resuspension of seabed material at the foot of the continental slope in the rockall channel. *Mar. Geol.* 2006 2/28;226(3-4):167-84.
- Bowie A.R., Sedwick P.N., Worsfold P.J. Analytical intercomparison between flow injection-chemiluminescence and flow injection-spectrophotometry for the determination of picomolar concentrations of iron in seawater. *Limnology and Oceanography: Methods* 2004;2:42-54.
- Bowie A.R., Achterberg E.P., Blain S., Boye M., Croot P.L., de Baar H.J.W., Laan P., Sarthou G., Worsfold P.J. Shipboard analytical intercomparison of dissolved iron in surface waters along a north-south transect of the Atlantic Ocean. *Mar. Chem.* 2003 12;84(1-2):19-34.
- Bowie A.R., Achterberg E.P., Croot P.L., de Baar H.J.W., Laan P., Moffett J.W., Ussher S., Worsfold P.J. A community-wide intercomparison exercise for the determination of dissolved iron in seawater. *Mar. Chem.* 2006 1/2;98(1):81-99.
- Bowie A.R., Achterberg E.P., Mantoura R.F.C., Worsfold P.J. Determination of sub-nanomolar levels of iron in seawater using flow injection with chemiluminescence detection. *Anal. Chim. Acta* 1998 4/17;361(3):189-200.
- Bowie A.R., Whitworth D.J., Achterberg E.P., Mantoura R.F.C., Worsfold P.J. Biogeochemistry of Fe and other trace elements (Al, Co, Ni) in the upper Atlantic ocean. *Deep Sea Research Part I: Oceanographic Research Papers* 2002 4;49(4):605-36.
- Brand L.E., Sunda W.G., Guillard R.R.L. Limitation of marine phytoplankton reproductive rates by zinc, manganese, and iron. *Limnology and Oceanography* 1983;28(6):1182-98.
- Breitbarth E., Bellerby R.J., Neill C.C., Ardelan M.V., Meyerhöfer M., Zöllner E., Croot P.L., Riebesell U. Ocean acidification affects iron speciation during a coastal seawater mesocosm experiment. *Biogeosciences* 2010;7:1065-73.
- Bruland K. W. and Rue E. L.. Analytical methods for the determination of concentrations and speciation of iron. In: David R. Turner, Keith A. Hunter, editors. *The biogeochemistry of iron in sea water*. IUPAC Series on Analytical and Physical Chemistry of Environmental Systems. Volume 7 ed. John Wiley & Sons Ltd; 2001.
- de Baar H. J. W. and de Jong J. T. M. Distributions, sources and sinks of iron in seawater. In: David R. Turner, Keith A. Hunter, editors. *The biogeochemistry of iron in sea water*. IUPAC Series on

Analytical and Physical Chemistry of Environmental Systems. Volume 7 ed. John Wiley & Sons Ltd; 2001.

Fitzwater S.E., Coale K.H., Gordon R.M., Johnson K.S., Ondrusek M.E. Iron deficiency and phytoplankton growth in the equatorial pacific. *Deep Sea Research Part II: Topical Studies in Oceanography* 1996;43(4–6):995-1015.

Fraille-Nuez E., González-Dávila M., Santana-Casiano J.M., Arístegui J., Alonso-González I.J., Hernández-León S., Blanco M.J., Rodríguez-Santana A., Hernández-Guerra A., Gelado-Caballero M.D., et al. The submarine volcano eruption at the island of El Hierro: Physical-chemical perturbation and biological response. *Scientific Reports* 2012;2:1-6.

Fu F., Mulholland M.R., Garcia N.S., Beck A., Bernhardt P.W., Warner M.E., Sañudo-Wilhelmy S.A., Hutchins D.A. Interactions between changing pCO₂, N₂ fixation, and Fe limitation in the marine unicellular cyanobacterium *crocosphaera*. *Limnology and Oceanography* 2008;53(6):2472-84.

Gledhill M., McCormack P., Ussher S., Achterberg E.P., Mantoura R.F.C., Worsfold P.J. Production of siderophore type chelates by mixed bacterioplankton populations in nutrient enriched seawater incubations. *Mar. Chem.* 2004 8;88(1–2):75-83.

González-Dávila M. The role of phytoplankton cells on the control of heavy metal concentration in seawater. *Mar. Chem.* 1995 2;48(3–4):215-36.

González-Davila M., Santana-Casiano J.M., Millero F.J. Competition between O₂ and H₂O₂ in the oxidation of Fe(II) in natural waters. *Journal of Solution Chemistry* 2006;35(1):95-111.

González-Davila M., Santana-Casiano J.M., Millero F.J. Oxidation of iron(II) nanomolar with H₂O₂ in seawater. *Geochim. Cosmochim. Acta* 2004 1/1;69(1):83-93.

Hansard S. Paul, Landing William M. Determination of iron(II) in acidified seawater samples by luminol chemiluminescence. *Limnology and Oceanography: Methods* 2009;7:222-34.

Hutchins D.A., Bruland K.W. Grazer-mediated regeneration and assimilation of Fe, Zn and Mn from planktonic prey. *Marine Ecology Progress Serie* 1994;110:259-69.

Jickells T. D. and Spokes L. J.. Atmospheric iron inputs to the ocean. In: David R. Turner, Keith A. Hunter, editors. *The biogeochemistry of iron in sea water*. IUPAC Series on Analytical and Physical Chemistry of Environmental Systems. Volume 7 ed. John Wiley & Sons Ltd; 2001.

Johnson K.S., Gordon R.M., Coale K.H. What controls dissolved iron concentrations in the world ocean? *Mar. Chem.* 1997 7;57(3–4):137-61.

King, D. Whitney and Farlow, R. Role of carbonate speciation on the oxidation of Fe(II) by H₂O₂. *Marine Chemistry* 2000;70:201-9.

King D.W., Lounsbury H.A., Millero F.J. Rates and mechanism of Fe(II) oxidation at nanomolar total iron concentrations. *Environmental Science and Technology* 1995;29(3):818-24.

Kustka A.B., Shaked Y., Milligan A.J., King D.W., Morel François M. M. Extracellular production of superoxide by marine diatoms: Contrasting effects on iron redox chemistry and bioavailability. *Limnology and Oceanography* 2005;50(4):1172-80.

Liu X., Millero F.J. The solubility of iron hydroxide in sodium chloride solutions. *Geochim. Cosmochim. Acta* 1999 10;63(19–20):3487-97.

- Liu X., Millero F.J. The solubility of iron in seawater. *Mar. Chem.* 2002 1;77(1):43-54.
- Mantas V.M., Pereira A.J.S.C., Morais P.V. Plumes of discolored water of volcanic origin and possible implications for algal communities. The case of the home reef eruption of 2006 (Tonga, southwest Pacific Ocean). *Remote Sens. Environ.* 2011 6/15;115(6):1341-52.
- Martin J.H., Coale K.H., Johnson K.S., Fitzwater S.E., Gordon R.M., Tanner S.J., Hunter C.N., Elrod V.A., Nowicki J.L., Coley T.L., et al. Testing the iron hypothesis in ecosystems of the equatorial Pacific Ocean. *Nature* 1994;371:123-9.
- Martin J.H., Gordon, R. Michael and Fitzwater, Steve E. Iron limitation? *Limnology and Oceanography* 1991;36(8):1793-802.
- Miller W.L., King D.W., Lin J., Kester D.R. Photochemical redox cycling of iron in coastal seawater. *Marine Chemistry* 1995;50:63-77.
- Millero F.J., Yao W., Aicher J. The speciation of Fe(II) and Fe(III) in natural waters. *Mar. Chem.* 1995 8;50(1-4):21-39.
- Nishioka J., Obata H., Tsumune D. Evidence of an extensive spread of hydrothermal dissolved iron in the Indian Ocean. *Earth Planet Sci. Lett.* 2013 1/1;361(0):26-33.
- O'Hara Murray R.B., Hodgson D.M., Thorne P.D. Wave groups and sediment resuspension processes over evolving sandy bedforms. *Cont. Shelf. Res.* 2012 9/1;46(0):16-30.
- O'Sullivan D.W., Hanson Jr. A.K., Kester D.R. Stopped flow luminol chemiluminescence determination of Fe(II) and reducible iron in seawater at subnanomolar levels. *Mar. Chem.* 1995 3;49(1):65-77.
- Powell R.T., King D.W., Landing W.M. Iron distributions in surface waters of the south Atlantic. *Mar. Chem.* 1995 8;50(1-4):13-20.
- Rijkenberg M.J.A., Powell C.F., Dall'Osto M., Nielsdottir M.C., Patey M.D., Hill P.G., Baker A.R., Jickells T.D., Harrison R.M., Achterberg E.P. Changes in iron speciation following a saharan dust event in the tropical north Atlantic ocean. *Mar. Chem.* 2008 5/16;110(1-2):56-67.
- Rose A.L., Waite T.D. Role of superoxide in the photochemical reduction of iron in seawater. *Geochimica Et Cosmochimica Acta* 2006;70:3869-82.
- Sander S.G., Koschinsky A. Metal flux from hydrothermal vents increased by organic complexation. *Nature Geoscience* 2011;4(MARCH 2011):145-50.
- Santana-Casiano J.M., González-Dávila M., Fraile-Nuez E., de Armas D., González A.G., Domínguez-Yanes J.F., Escáñez J. The natural ocean acidification and fertilization event caused by the submarine eruption of El Hierro. *Scientific Reports* 2013;3:1-8.
- Santana-Casiano J.M., González-Dávila M., Millero F.J. The role of Fe(II) species on the oxidation of Fe(II) in natural waters in the presence of O₂ and H₂O₂. *Mar. Chem.* 2006 3/6;99(1-4):70-82.
- Santana-Casiano J.M., González-Dávila M., Millero F.J. Comment on "Oxygenation of Fe(II) in natural waters revisited: Kinetic modeling approaches, rate constant estimation and the importance of various reaction pathways" by Pham and Waite (2008). *Geochim. Cosmochim. Acta* 2010 9/1;74(17):5150-3.

- Santana-Casiano J.M., González-Dávila M., Laglera L.M., Pérez-Peña J., Brand L., Millero F.J. The influence of zinc, aluminum and cadmium on the uptake kinetics of iron by algae. *Mar. Chem.* 1997 12;59(1–2):95-111.
- Santana-Casiano J.M., González-Dávila M., Millero F.J. The oxidation of Fe(II) in NaCl–HCO₃[–] and seawater solutions in the presence of phthalate and salicylate ions: A kinetic model. *Mar. Chem.* 2004 2;85(1–2):27-40.
- Santana-Casiano J.M., González-Dávila M., Rodríguez M.J., Millero F.J. The effect of organic compounds in the oxidation kinetics of Fe(II). *Marine Chemistry* 2000;70:211-22.
- Sarthou G., Baker A.R., Blain S., Achterberg E.P., Boye M., Bowie A.R., Croot P., Laan P., de Baar H.J.W., Jickells T.D., et al. Atmospheric iron deposition and sea-surface dissolved iron concentrations in the eastern Atlantic ocean. *Deep Sea Research Part I: Oceanographic Research Papers* 2003 0;50(10–11):1339-52.
- Severmann S., Johnson C.M., Beard B.L., German C.R., Edmonds H.N., Chiba H., Green D.R.H. The effect of plume processes on the Fe isotope composition of hydrothermally derived Fe in the deep ocean as inferred from the rainbow vent site, mid-Atlantic ridge, 36°14'N. *Earth Planet Sci. Lett.* 2004 8/30;225(1–2):63-76.
- Shi D., Xu Y., Brian M.H., Morel François M. M. Effect of ocean acidification on iron availability to marine phytoplankton. *Science* 2010;327:676-9.
- Spokes L., Jickells T., Jarvis K. Atmospheric inputs of trace metals to the northeast Atlantic ocean: The importance of southeasterly flow. *Marine Chemistry* 2001;76:319-30.
- Statham P.J., German C.R., Connelly D.P. Iron (II) distribution and oxidation kinetics in hydrothermal plumes at the Kairei and Edmond vent sites, Indian ocean. *Earth Planet Sci. Lett.* 2005 8/15;236(3–4):588-96.
- Sunda W. G. Bioavailability and bioaccumulation of iron in the sea. In: David R. Turner, Keith A. Hunter, editors. *The biogeochemistry of iron in sea water. IUPAC Series on Analytical and Physical Chemistry of Environmental Systems. Volume 7 ed.* John Wiley & Sons Ltd; 2001. .
- Turner D. R., Hunter K. A. and de Baar H. J. W.. Introduction. In: David R. Turner, Keith A. Hunter, editors. *The biogeochemistry of iron in sea water. IUPAC Series on Analytical and Physical Chemistry of Environmental Systems. Volume 7 ed.* John Wiley & Sons Ltd; 2001.
- Trapp J.M., Millero F.J. The oxidation of iron(II) with oxygen in NaCl brines. *J. Solution Chem.* 2007;36:1479-93.
- Ussher S.J., Achterberg E.P., Sarthou G, Laan P, de Baar HJW, Worsfold PJ. Distribution of size fractionated dissolved iron in the canary basin. *Mar. Environ. Res.* 2010 7;70(1):46-55.
- Waite T. D.. Thermodynamics of the iron system in seawater. In: David R. Turner, Keith A. Hunter, editors. *The biogeochemistry of iron in sea water. IUPAC Series on Analytical and Physical Chemistry of Environmental Systems. Volume 7 ed.* John Wiley & Sons Ltd; 2001.
- Ye Y., Völker C. and Wolf-Gladrow, D. A. A model of Fe speciation and biogeochemistry at the tropical eastern north Atlantic time-series observatory site. *Biogeosciences* 2009;6(10):2041-61.
- Zhang F., Reeks M.W., Kissane M.P., Perkins R.J. Resuspension of small particles from multilayer deposits in turbulent boundary layers. *J. Aerosol Sci.* 2013 12;66(0):31-61.